

1 *In silico* candidate variant and gene 2 identification using inbred mouse strains

3 Matthias Munz^{1*}, Mohammad Khodaygani^{1*}, Zouhair Aherrahrou², Hauke
4 Busch^{1#}, and Inken Wohlers^{1#}

5 ¹Medical Systems Biology Division, Lübeck Institute of Experimental Dermatology and
6 Institute for Cardiogenetics, University of Lübeck, Lübeck, Germany

7 ²Institute for Cardiogenetics, University of Lübeck, Lübeck, Germany

8 *,#These authors contributed equally

9 Corresponding author:

10 Hauke Busch and Inken Wohlers

11 Email address: hauke.busch@uni-luebeck.de and inken.wohlers@uni-luebeck.de

12 ABSTRACT

13 Mice are the most widely used animal model to study genotype to phenotype relationships. Inbred mice
14 are genetically identical, which eliminates genetic heterogeneity and makes them particularly useful for
15 genetic studies. Many different strains have been bred over decades and a vast amount of phenotypic
16 data has been generated. In addition, lately, also whole genome sequencing-based genome-wide
17 genotype data for many widely used inbred strains has been released. Here, we present an approach
18 for *in silico* fine mapping that uses genotypic data of 37 inbred mouse strains together with phenotypic
19 data provided by the user to propose candidate variants and genes for the phenotype under study. Public
20 genome-wide genotype data covering more than 74 million variant sites is queried efficiently in real-time
21 to provide those variants that are compatible with the observed phenotype differences between strains.
22 Variants can be filtered by molecular consequences and by corresponding molecular impact. Candidate
23 gene lists can be generated from variant lists on the fly. Fine mapping together with annotation or filtering
24 of results is provided in a Bioconductor package called MouseFM. For albinism, MouseFM reports only
25 one variant allele of moderate or high molecular impact that only albino mice share: a missense variant
26 in the *Tyr* gene, reported previously to be causal for this phenotype. Performing *in silico* fine mapping for
27 interfrontal bone formation in mice using four strains with and five strains without interfrontal bone results
28 in 12 genes. Of these, three are related to skull shaping abnormality. Finally performing fine mapping for
29 dystrophic cardiac calcification by comparing 8 strains showing the phenotype with 8 strains lacking it, we
30 identify only one moderate impact variant in the known causal gene *Abcc6*. In summary, this illustrates
31 the benefit of using MouseFM for candidate variant and gene identification.

32 INTRODUCTION

33 Mice are the most widely used animal models in research. Several factors such as small size, low cost
34 of maintain, and fast reproduction as well as sharing disease phenotypes and physiological similarities
35 with human makes them one of the most favourable animal model (Uhl and Warner, 2015). Inbred mouse
36 strains are strains with all mice being genetically identical, i.e. clones, as a result of sibling mating for
37 many generations, which results in eventually identical chromosome copies. When assessing genetic
38 variance between mouse strains, the genome of the most commonly used inbred strain, called black 6
39 (C57BL/6J) is typically used as reference and variants called with respect to the black 6 mouse genome.
40 For inbred mouse strains, variants are homozygous by design.

41 Grupe *et al.* in 2001 published impressive results utilizing first genome-wide genetic data for *in*
42 *silico* fine mapping of complex traits, “reducing the time required for analysis of such [inbred mouse]
43 models from many months down to milliseconds” (Grupe *et al.*, 2001). Darvasi commented on this paper
44 that in his opinion, the benefit of *in silico* fine mapping lies in the analysis of monogenic traits and in
45 informing researchers prior to initiating traditional breeding-based studies. In 2007, with Cervino *et al.*,
46 he suggested to combine *in silico* mapping with expression information for gene prioritization using

47 20,000 and 240,000 common variants, respectively (Cervino et al., 2007). Although genetic data improved
 48 incredibly since then – now all genetic variation between all commonly used inbred strains is known at
 49 base pair resolution (Doran et al., 2016) (Keane et al., 2011) – to the best of our knowledge, the idea of *in*
 50 *silico* fine mapping using inbred mouse strains has not been picked up again since then.

51 At the same time, in the last years huge amounts of mouse phenotype data were generated, often
 52 in collaborative efforts and systematically for many mouse strains. Examples are phenotyping under-
 53 taken by the International Mouse Phenotyping Consortium (IMPC) (Dickinson et al., 2016)(Meehan
 54 et al., 2017) or lately also the phenotyping of the expanded BXD family of mice (Ashbrook et al.,
 55 2019). Data are publicly available in resources such as the mouse phenotype database (MPD) (Bogue
 56 et al., 2018) (<https://www.mousephenotype.org>) or the IMPC’s website (Dickinson et al.,
 57 2016) (<https://phenome.jax.org>). Other websites such as Mouse Genome Informatics (MGI)
 58 (<http://www.informatics.jax.org>) or GeneNetwork (Mulligan et al., 2017) (<https://www.genenetwork.org>) also house phenotype data together with web browser-based functionality to in-
 59 vestigate genotype-phenotype relationships.

61 Several of the aforementioned resources allow to interactively query genotypes for user-selected inbred
 62 mouse strains for input genes or genetic regions. None of them though provides the functionality to extract
 63 genome-wide all variants that are different between two user-specified groups of inbred mouse strains.
 64 Such information can be used for *in silico* fine mapping and for the identification of candidate genes and
 65 variants underlying a phenotypic trait. Further, such a catalog of genetic differences between groups of
 66 strains is very useful prior to designing mouse breeding-based experiments e.g. for the identification or
 67 fine mapping of quantitative trait loci (QTL).

68 METHODS

69 Fine mapping approach

70 Unlike previous approaches for *in silico* fine mapping, here we are using whole genome sequencing-based
 71 variant data and thus information on all single nucleotide variation present between inbred strains. Due to
 72 the completeness of this variant data, we do not need to perform any statistical aggregation of variant data
 73 over genetic loci, but simply report all variant sites with different alleles between two groups of inbred
 74 strains. That is, we report all variant sites with alleles compatible with the observed phenotype difference,
 75 see Figure 1 for an illustration.

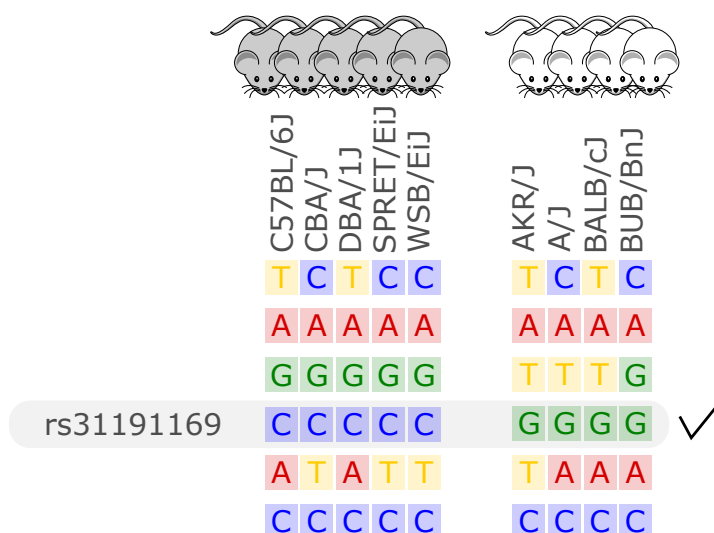


Figure 1. Illustration of the *in silico* fine mapping approach. Every row represents a variant site and every column one inbred mouse strain. In this example, the phenotype is albinism and four strains are albinos and 5 are not. Displayed are six variants, but only one variant, rs31191169, has consistently different alleles between the albino and the other mice (G allele is here linked to albinism). With option `thr2=1` in the MouseFM package, one discordant strain would be allowed in the second strain group and the variant in the row above rs31191169 would also be returned.

76 In the case of a binary phenotype caused by a single variant, this causal variant is one of the variants
77 that has a different allele in those strains showing the phenotype compared to those strains lacking the
78 phenotype. This is the case for example for albinism and its underlying causal variant rs31191169, used
79 in Figure 1 for illustration and discussed later in detail.

80 This *in silico* fine mapping approach can reduce the number of variants to a much smaller set of
81 variants that are compatible with a phenotype. The more inbred strains are phenotyped and used for
82 comparison, the more variants can be discarded because they are not compatible with the observed
83 phenotypic difference.

84 In the case of a quantitative phenotype, the fine mapping can be performed in two ways. The first
85 option is to obtain genetic differences between strains showing the most extreme phenotypes. The second
86 option is binarization of the phenotype by applying a cutoff. Since in these cases allele differences of
87 variants affecting the trait may not be fully compatible with an artificially binarized phenotype, fine
88 mapping is provided with an option that allows alleles of a certain number of strains to be incompatible
89 with the phenotype, see Figure 1 for an example.

90 Variant data

91 The database used by this tool was created based on the genetic variants database of the Mouse Genomes
92 Project (<https://www.sanger.ac.uk/science/data/mouse-genomes-project>) of the
93 Wellcome Sanger Institute. It includes whole genome sequencing-based single nucleotide variants of
94 36 inbred mouse strains which have been compiled by Keane et al. (2011), see ftp://ftp-mouse.sanger.ac.uk/REL-1502-BAM/sample_accessions.txt for the accession code and sources.
95 This well designed set of inbred mouse strains for which genome-wide variant data is available in-
96 cludes classical laboratory strains (C3H/HeJ, CBA/J, A/J, AKR/J, DBA/2J, LP/J, BALB/cJ, NZO/HILtJ,
97 NOD/ShiLtJ), strains extensively used in knockout experiments (129S5SvEvBrd, 129P2/OlaHsd, 129S1/SvImJ,
98 C57BL/6NJ), strains used commonly for a range of diseases (BUB/BnJ, C57BL/10J, C57BR/cdJ, C58/J,
99 DBA/1J, I/LnJ, KK/HiJ, NZB/B1NJ, NZW/LacJ, RF/J, SEA/GnJ, ST/bJ) as well as wild-derived inbred
100 strains from different mouse taxa (CAST/EiJ, PWK/PhJ, WSB/EiJ, SPRET/EiJ, MOLF/EiJ). Genome se-
101 quencing, variant identification and characterization of 17 strains was performed by Keane et al. (2011) and
102 of 13 strains by Doran et al. (2016). We downloaded the single nucleotide polymorphism (SNP) VCF file
103 ftp://ftp-mouse.sanger.ac.uk/current_snps/mgp.v5.merged.snps_all.dbSNP142.vcf.gz. Overall, it contains 78,767,736 SNPs, of which 74,873,854 are autosomal. The chromosomal
104 positions map to the mouse reference genome assembly GRCm38 which is based on the C57 black 6
105 inbred mouse strain and by definition has no variant positions.

106 Low confidence, heterozygous, missing and multiallelic variants vary by strain, in sum they are
107 typically less than 5% of the autosomal variants (Figure 2, Suppl. Table 1). Exceptions are for example the
108 wild-derived inbred strains, for which variant genotypes excluded from the database reach a maximum of
109 11.5% for SPRET/EiJ. There are four strains that are markedly genetically different from each other and
110 all remaining strains, these are the wild-derived, inbred strains CAST/EiJ, PWK/PhJ, SPRET/EiJ and
111 MOLF/EiJ, see Figure 2A. These four strains also show the highest number of missing and multiallelic
112 genotypes (Figure 2B and Suppl. Table 1).
113
114

115 Database

116 We re-annotated the source VCF file with Ensembl Variant Effect Predictor (VEP) v100 (McLaren
117 et al., 2016) using a Docker container image (<https://github.com/matmu/vep>). For real-time
118 retrieval of variants compatible with phenotypes under various filtering criteria, the variant data was
119 loaded into a MySQL database. The database consists of a single table with columns for chromosomal
120 locus, the reference SNP cluster ID (rsID), variant consequences based on a controlled vocabulary from
121 the sequence ontology (Eilbeck et al., 2005), the consequence categorization into variant impacts “HIGH”,
122 “MODERATE”, “LOW” or “MODIFIER” according to the Ensembl Variation database (Hunt et al., 2018)
123 (see Suppl. Table 2 for details) and the genotypes (NULL = missing, low confidence, heterozygous or
124 consisting of other alleles than reference or most frequent alternative allele; 0 = homozygous for the
125 reference allele, 1 = homozygous for alternative allele). SNPs with exclusively NULL genotypes were not
126 loaded into the database resulting in 74,480,058 autosomal SNVs that were finally added to our database.
127 These have been annotated with overall 120,927,856 consequences, i.e. on average every variant has
128 two annotated consequences. Figure 3 summarizes these consequence annotations stratified by impact;
129 description of consequences and annotation counts are provided in Suppl. Table 2. Most annotations

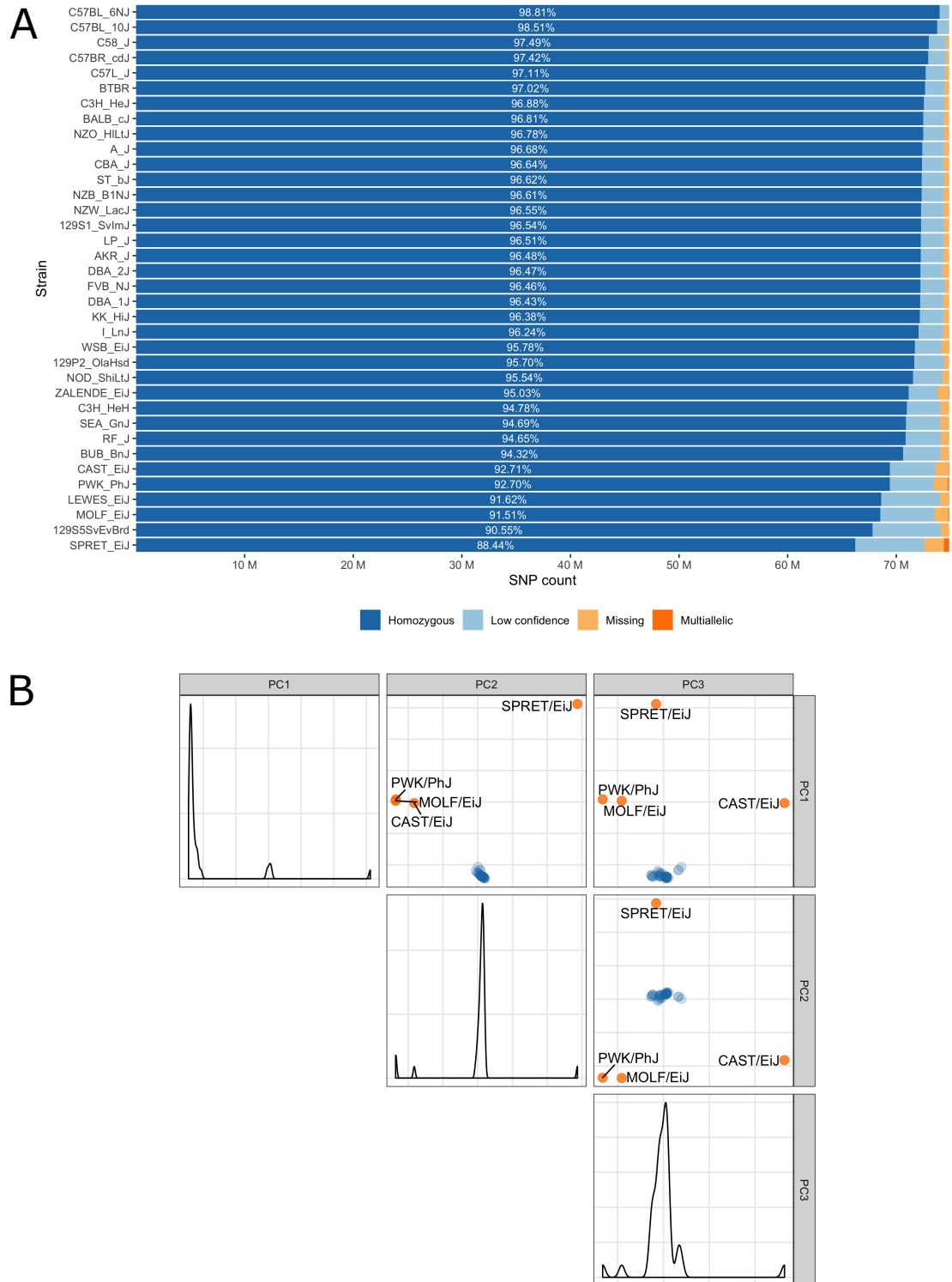


Figure 2. A) Inbred mouse strain autosomal SNP characteristics: The number of homozygous, low confidence, missing and multiallelic genotypes for 36 non-reference strains. For each strain, a SNP was checked for group membership in the order low confidence → missing → multiallelic → homozygous → heterozygous and was assigned to the first matching group. Since no SNP made it to the group with heterozygous genotypes it is not shown in the diagram. B) Principal component analysis shows four outlier inbred strains, CAST/EiJ, PWK/PhJ, SPRET/EiJ and MOLF/EiJ.

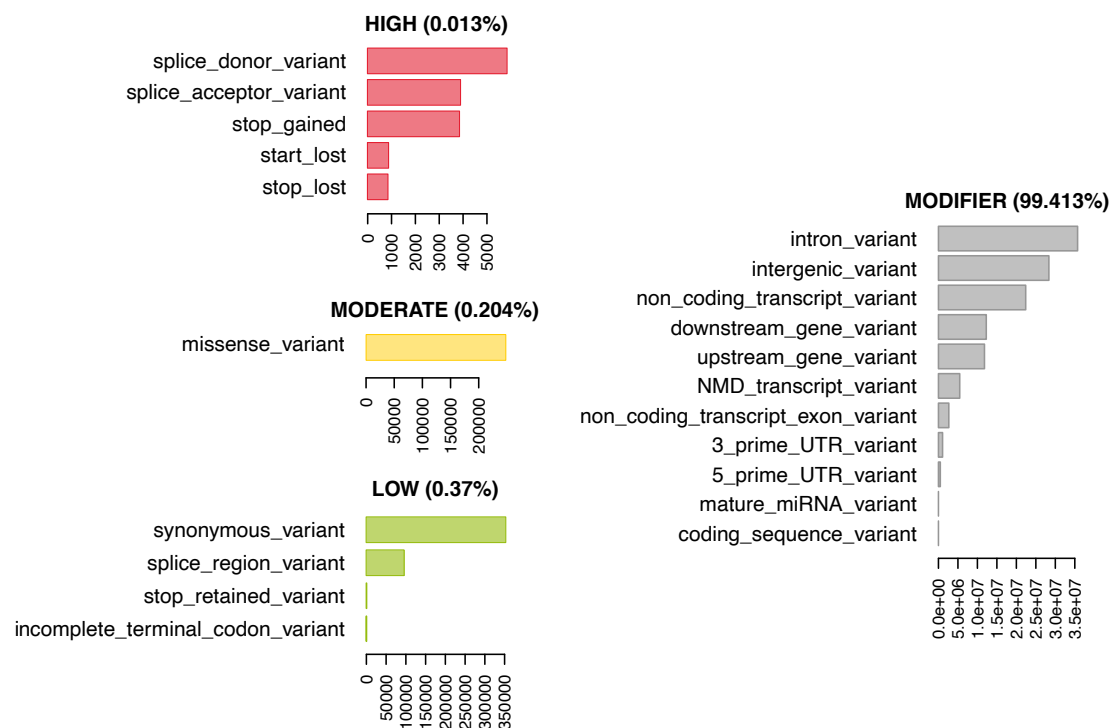


Figure 3. 74,480,058 variants have been annotated with 120,927,856 consequences. Shown here are the number of variants annotated with a given consequence, stratified by consequence impact (“HIGH”, “MODERATE”, “LOW”, “MODIFIER”). For description of consequence types see Suppl. Table 2. Both impact and consequence can be used for variant prioritization in MouseFM.

130 belong to impact category “MODIFIER” (99.4%). High impact annotations are rare, because they are
 131 typically deleterious (0.013%). Annotation with moderate impact consequences comprise only missense,
 132 i.e. protein sequence altering variants contributing 0.204%. Low impact consequences are slightly more
 133 often annotated, amounting to 0.37%.

134 **Bioconductor R package MouseFM**

135 Our fine mapping approach was implemented as function `finemap` in the Bioconductor R package
 136 “MouseFM”. Bioconductor is a repository for open software for bioinformatics.

137 Function `finemap` takes as input two groups of inbred strains and one or more chromosomal
 138 regions on the GRCm38 assembly and returns a SNP list for which the homozygous genotypes are
 139 discordant between the two groups. Optionally, filters for variant consequence and impacts as well
 140 as a threshold for each group to allow for intra-group discordances can be passed. With function
 141 `annotate_mouse_genes` the SNP list can further be annotated with overlapping genes. Optionally,
 142 flanking regions can be passed.

143 The `finemap` function queries the genotype data from our backend server while function `annotate_mouse_genes`
 144 queries the Ensembl Rest Service (Yates et al., 2014). The repository containing the backend of the
 145 MouseFM tool, including the scripts of the ETL (Extract, transform, load) process and the webserver,
 146 is available at <https://github.com/matmu/MouseFM-Backend>. Following the repositories’
 147 instructions, users may also install the data base and server application on a local server.

148 **RESULTS**

149 As a proof of concept, we applied our *in silico* fine mapping approach on three phenotypes: albinism,
 150 interfrontal bone formation and dystrophic cardiac calcification. Phenotypic data is illustrated in Figure 4.

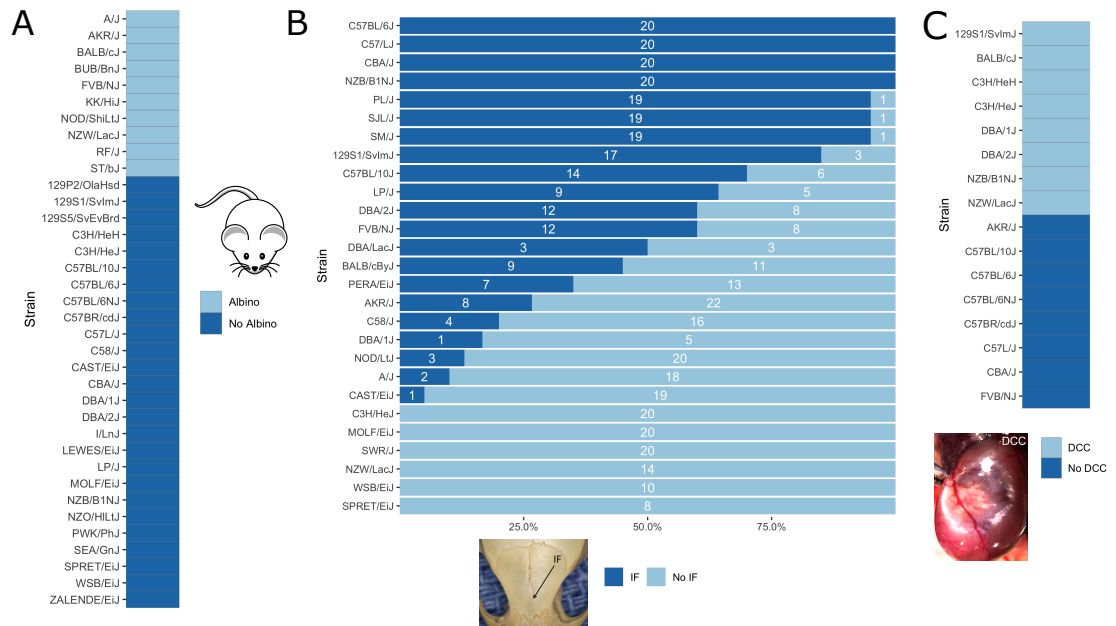


Figure 4. Visualization of mouse phenotypic data for which fine mapping is performed. A) Binary inbred mouse strain phenotype albinism. All or no mice of a strain are albinos; shown here is which strain belongs to which group. B) Quantitative inbred mouse strain phenotype interfrontal bone (IF). Shown is the number of mice of the respective strain having an interfrontal bone (dark blue, IF) and not having an interfrontal bone (light blue, No IF). The interfrontal bone (IF) image is taken from (Zimmerman et al., 2019).

Albinism

Albinism is the absence of pigmentation resulting from a lack of melanin and is well-studied in mice (Beermann et al., 2004). It is a monogenic trait caused by a mutation in the *Tyr* gene (Beermann et al., 2004), which encodes for tyrosinase, an enzyme involved in melanin synthesis. The *Tyr* locus has been used before for the validation of *in silico* fine mapping approaches (Cervino et al., 2007). According to the Jackson Laboratory website (<https://www.jax.org>), 10 of the 37 inbred mouse strains are albinos with a *Tyr^c* genotype (<http://www.informatics.jax.org/allele/MGI:1855976>), see Figure 4A.

Our algorithm resulted in only one genetic locus, which includes the *Tyr* gene; only 245 SNPs have different alleles between the albino and non-albino inbred mouse strains, all located from 7:83,244,464 to 7:95,801,713 (GRCm38). When removing SNPs except those of moderate or high impact, only one variant remains. This variant rs31191169 at position 7:87,493,043, with reference allele C and with alternative allele G in the albino strains is the previously described causal missense SNP in the *Tyr* gene, which results in a cysteine to serine amino acid change at position 103 of the tyrosine protein.

Interfrontal bone

Further, we applied our algorithm on the phenotype of interfrontal bone formation, a complex skeletal trait residing between the frontal bones in inbred mice (Figure 4B). In some inbred mouse strains, the interfrontal bone is present or absent in all mice, whereas other strains are polymorphic for this phenotype suggesting that phenotypic plasticity is involved. Phenotypic data related to interfrontal bone has recently been generated by Zimmerman *et al.* (Zimmerman et al., 2019) for 27 inbred mouse strains (Figure 4B). They performed QTL mapping and identified four significant loci on chromosomes 4,7,11 and 14, the same loci for interfrontal bone length and interfrontal bone width. For the genotyping, the authors use the mapping and developmental analysis panel (MMDAP; Partners HealthCare Center for Personalized Genetic Medicine, Cambridge, MA, United States), which contains 748 SNPs.

Of the available interfrontal bone data, we only used inbred strains for which all mice show the same phenotype. This corresponds to four strains with interfrontal bone (C57BL/6J, C57L/J, CBA/J,

177 NZB/B1NJ) and five strains without interfrontal bone (C3H/HEJ, MOLF/EiJ, NZW/LacJ, WSB/EiJ,
178 SPRET/EiJ).

179 *In silico* fine mapping resulted in 8,608 SNPs compatible with the observed interfrontal bone pheno-
180 type. Of these, 15 showed moderate or high impact on 12 candidate genes, see Table 1. None of the loci
181 identified by us overlaps with the fine mapping results reported by Zimmerman *et al.* Variant rs29393437
182 is located in the less well described isoform ENSMUST00000131519.1 of *Stac2*, one of two isoforms of
183 this gene. It is a missense variant, changing arginine (R) to histidine (H) which is at low confidence
184 predicted to be deleterious by SIFT. *Stac2* has been shown to negatively regulate formation of osteoclasts,
185 cells that dissect bone tissue (Jeong *et al.*, 2018). *Phf21* is expressed during ossification of cranial bones in
186 mouse early embryonic stages and has been linked to craniofacial development (Kim *et al.*, 2012). Gene
187 *Abcc6* is linked to abnormal snout skin morphology in mouse and abnormality of the mouth, high palate
188 in human according to MGI.

RSID	Position	Gene
rs32785405	1:36311963	<i>Arid5a</i>
rs27384937	2:92330761	<i>Phf21a</i>
rs32757904	7:45996764	<i>Abcc6</i>
rs32761224	7:46068710	<i>Nomo1</i>
rs32763636	7:46081416	<i>Nomo1</i>
rs13472312	7:46376829	<i>Myod1</i>
rs31674298	7:46443316	<i>Sergef</i>
rs31226051	7:49464827	<i>Nav2</i>
rs248206089	7:49547983	<i>Nav2</i>
rs45995457	9:86586988	<i>Me1</i>
rs29393437	11:98040971	<i>Stac2</i>
rs29414131	11:98042573	<i>Stac2</i>
rs251305478	11:98155926	<i>Med1</i>
rs27086373	11:98204403	<i>Cdk12</i>
rs27026064	11:98918145	<i>Cdc6</i>

Table 1. Moderate and high impact candidate variants and genes for interfrontal bone formation.

189 **Dystrophic cardiac calcification**

190 Physiological calcification takes place in bones, however pathologically calcification may affect the
191 cardiovascular system including vessels and the cardiac tissue. Dystrophic cardiac calcification (DCC) is
192 known as calcium phosphate deposits in necrotic myocardial tissue independently from plasma calcium
193 and phosphate imbalances. We previously reported the identification of four DCC loci *Dyscal1*, *Dyscal2*,
194 *Dyscal3*, and *Dyscal4* on chromosomes 7, 4, 12 and 14, respectively using QTL analysis and composite
195 interval mapping (Ivandic *et al.*, 1996, 2001). The *Dyscal1* was confirmed as major genetic determinant
196 contributing significantly to DCC (Aherrahrou *et al.*, 2004). It spans a 15.2 Mb region on proximal
197 chromosome 7. Finally, chromosome 7 was further refined to a 80 kb region and *Abcc6* was identified
198 as causal gene (Meng *et al.*, 2007; Aherrahrou *et al.*, 2007). In this study we applied our algorithm to
199 previously reported data on 16 mouse inbred strains which were well-characterized for DCC (Aherrahrou
200 *et al.*, 2007). Eight inbred mouse strains were found to be susceptible to DCC (C3H/HeJ, NZW/LacJ,
201 129S1/SvImJ, C3H/HeH, DBA/1J, DBA/2J, BALB/cJ, NZB/B1NJ) and eight strains were resistant to
202 DCC (CBA/J, FVB/NJ, AKR/J, C57BL/10J, C57BL/6J, C57BL/6NJ, C57BR/cdJ, C57L/J). 2,003 SNPs
203 in 13 genetic loci were fine mapped and found to match the observed DCC phenotype in the tested
204 16 DCC strains. Of these, 19 SNPs are moderate or high impact variants affecting protein amino acid
205 sequences of 13 genes localized in two chromosomal regions mainly on chromosome 7 (45.6-46.3 Mb)
206 and 11 (102.4-102.6 Mb), see Table 2. The SNP rs32753988 is compatible with the observed phenotype
207 manifestations and affects the previously identified causal gene *Abcc6*. This SNP has a SIFT score of 0.22,
208 the lowest score after two SNPs in gene *Sec1* and one variant in gene *Mamstr*, although SIFT predicts all
209 amino acid changes to be tolerated.

RSID	Position	Gene
rs46174746	7:45538428	<i>Plekha4</i>
rs49200743	7:45634990	<i>Rasip1</i>
rs32122777	7:45642384	<i>Mamstr</i>
rs215144870	7:45679109	<i>Sec1</i>
rs45768641	7:45679410	<i>Sec1</i>
rs51645617	7:45679423	<i>Sec1</i>
rs31997402	7:45725284	<i>Spaca4</i>
rs50753342	7:45794044	<i>Lmtk3</i>
rs50693551	7:45794821	<i>Lmtk3</i>
rs52312062	7:45798406	<i>Lmtk3</i>
rs49106901	7:45798469	<i>Emp3</i>
rs47934871	7:45918097	<i>Emp3</i>
rs32444059	7:45942897	<i>Ccdc114</i>
rs32753988	7:45998774	<i>Abcc6</i>
rs32778283	7:46219386	<i>Ush1c</i>
rs31889971	7:46288929	<i>Otog</i>
rs50613184	11:102456258	<i>Itga2b</i>
rs27040377	11:102457490	<i>Itga2b</i>
rs29383996	11:102605308	<i>Fzd2</i>

Table 2. Moderate and high impact candidate variants and genes for dystrophic cardiac calcification.

DISCUSSION & CONCLUSIONS

With MouseFM, we developed a novel tool for *in silico*-based genetic fine mapping exploiting the extremely high homozygosity rate of inbred mouse strains for identifying new candidate SNPs and genes. By including genotype data for 37 inbred mouse strains at a genome-wide scale derived from Next Generation Sequencing, MouseFM clearly outperforms earlier approaches.

By re-analyzing previously published fine mapping studies for albinism and dystrophic cardiac calcification, we could show that MouseFM is capable of re-identifying causal SNPs and genes. Re-analyzing a study on interfrontal bone formation (IF), however, did not show any overlap with the regions suggested in the original publication. Reasons might be complex nature of this phenotype and that the causal genetic factors are still largely unknown. With gene *Stac2* we suggest a new candidate gene possibly affecting interfrontal bone formation.

We observe that frequently genetic loci identified by MouseFM fine mapping consist of few or often only a single variant compatible with the phenotype. For example, five of 13 fine mapped DCC loci comprise a single phenotype-pattern compatible variant and 3 loci comprise less than 10 variants. This contradicts the expectation that commonly used mice strains differ by chromosomal segments comprising several or many consecutive variants. Commonly used inbred strains display mosaic genomes with sequences from different subspecific origins Wade et al. (2002) and thus one may expect genomic regions with high SNP rate. Fine mapped loci comprising more phenotype-compatible variants are thus likely more informative for downstream experiments. When allowing no phenotype outlier strain (i.e. $\text{thr1}=0$ and $\text{thr2}=0$), in the case of DCC we identify only six such genetic loci that lend themselves for further experimental fine mapping (chr7:45,327,763-46,308,368 (811 compatible SNVs); chr7:54,894,131-54,974,260 (32 compatible SNVs); chr9:106,456,180-106,576,076 (170 SNVs); chr11:24,453,006-24,568,761 (40 compatible SNVs); chr11:102,320,611-102,607,848 (46 compatible SNVs); chr16:65,577,755-66,821,071 (890 compatible SNVs)).

We show here that *in silico* fine mapping can effectively identify genetic loci compatible with the observed phenotypic differences and prioritize genetic variants and genes for further consideration. This allows for subsequent more targeted approaches towards identification of causal variants and genes using literature, data integration, and lab and animal experiments. MouseFM *in silico* fine mapping provides phenotype-compatible genotypic differences between representatives of many common laboratory mice strains. These genetic differences can be used to select strains which are genetically diverse at an indicated genetic locus and which are thus providing additional information when performing phenotyping or

241 breeding-based mouse experiments. Thus *in silico* fine mapping is a first, very efficient step on the way of
242 unraveling genotype-phenotype relationships.

243 During the implementation of MouseFM we have paid attention to a very easy handling. To perform a
244 fine mapping study, our tool only requires binary information (e.g. case versus control) for a phenotype of
245 interest on at least two of the 37 available input strains. Further optional parameters can be set to reduce
246 or expand the search space. MouseFM can also be performed on quantitative traits as we showed in the
247 interfrontal bone example.

248 In conclusion, MouseFM implements a conceptually simple, but powerful approach for *in silico* fine
249 mapping including a very comprehensive SNP set of 37 inbred mouse strains. By re-analyzing three fine
250 mapping studies, we demonstrate that MouseFM is a very useful tool for studying genotype-phenotype
251 relationships in mice.

252 ACKNOWLEDGEMENTS

253 MM, HB and IW acknowledge funding by the Deutsche Forschungsgemeinschaft (DFG, German Re-
254 search Foundation) under EXC 22167-390884018 and KFO 303 grant number BU 2487/3. All authors
255 acknowledge computational support from the OMICS compute cluster at the University of Lübeck.

256 REFERENCES

- 257 Aherrahrou, Z., Axtner, S. B., Kaczmarek, P. M., Jurat, A., Korff, S., Doehring, L. C., Weichenhan, D.,
258 Katus, H. A., and Ivandic, B. T. (2004). A locus on chromosome 7 determines dramatic up-regulation
259 of osteopontin in dystrophic cardiac calcification in mice. *The American Journal of Pathology*,
260 164(4):1379–1387.
- 261 Aherrahrou, Z., Doehring, L. C., Kaczmarek, P. M., Liptau, H., Ehlers, E.-M., Pomarino, A., Wrobel,
262 S., Götz, A., Mayer, B., Erdmann, J., and Schunkert, H. (2007). Ultrafine mapping of *Dyscalc1* to
263 an 80-kb chromosomal segment on chromosome 7 in mice susceptible for dystrophic calcification.
264 *Physiological Genomics*, 28(2):203–212.
- 265 Ashbrook, D. G., Arends, D., Prins, P., Mulligan, M. K., Roy, S., Williams, E. G., Lutz, C. M., Valenzuela,
266 A., Bohl, C. J., Ingels, J. F., McCarty, M. S., Centeno, A. G., Hager, R., Auwerx, J., Sen, S., Lu, L.,
267 and Williams, R. W. (2019). The expanded BXD family of mice: A cohort for experimental systems
268 genetics and precision medicine. *bioRxiv*, page 672097.
- 269 Beermann, F., Orlow, S. J., and Lamoreux, M. L. (2004). The Tyr (albino) locus of the laboratory
270 mouse. *Mammalian Genome: Official Journal of the International Mammalian Genome Society*,
271 15(10):749–758.
- 272 Bogue, M. A., Grubb, S. C., Walton, D. O., Philip, V. M., Kolishovski, G., Stearns, T., Dunn, M. H.,
273 Skelly, D. A., Kadakkuzha, B., TeHennepe, G., Kunde-Ramamoorthy, G., and Chesler, E. J. (2018).
274 Mouse Phenome Database: an integrative database and analysis suite for curated empirical phenotype
275 data from laboratory mice. *Nucleic Acids Research*, 46(D1):D843–D850.
- 276 Cervino, A. C. L., Darvasi, A., Fallahi, M., Mader, C. C., and Tsinoremas, N. F. (2007). An integrated *in*
277 *silico* gene mapping strategy in inbred mice. *Genetics*, 175(1):321–333.
- 278 Dickinson, M. E., Flenniken, A. M., Ji, X., Teboul, L., Wong, M. D., White, J. K., Meehan, T. F., Weninger,
279 W. J., Westerberg, H., Adissu, H., Baker, C. N., Bower, L., Brown, J. M., Caddle, L. B., Chiani, F., Clary,
280 D., Cleak, J., Daly, M. J., Denegre, J. M., Doe, B., Dolan, M. E., Edie, S. M., Fuchs, H., Gailus-Durner,
281 V., Galli, A., Gambadoro, A., Gallegos, J., Guo, S., Horner, N. R., Hsu, C.-W., Johnson, S. J., Kalaga,
282 S., Keith, L. C., Lanoue, L., Lawson, T. N., Lek, M., Mark, M., Marschall, S., Mason, J., McElwee,
283 M. L., Newbigging, S., Nutter, L. M. J., Peterson, K. A., Ramirez-Solis, R., Rowland, D. J., Ryder, E.,
284 Samocho, K. E., Seavitt, J. R., Selloum, M., Szoke-Kovacs, Z., Tamura, M., Trainor, A. G., Tudose,
285 I., Wakana, S., Warren, J., Wendling, O., West, D. B., Wong, L., Yoshiki, A., International Mouse
286 Phenotyping Consortium, Jackson Laboratory, Infrastructure Nationale PHENOMIN, Institut Clinique
287 de la Souris (ICS), Charles River Laboratories, MRC Harwell, Toronto Centre for Phenogenomics,
288 Wellcome Trust Sanger Institute, RIKEN BioResource Center, MacArthur, D. G., Tocchini-Valentini,
289 G. P., Gao, X., Flicek, P., Bradley, A., Skarnes, W. C., Justice, M. J., Parkinson, H. E., Moore, M.,
290 Wells, S., Braun, R. E., Svenson, K. L., de Angelis, M. H., Herault, Y., Mohun, T., Mallon, A.-M.,
291 Henkelman, R. M., Brown, S. D. M., Adams, D. J., Lloyd, K. C. K., McKerlie, C., Beaudet, A. L.,

- 292 Bućan, M., and Murray, S. A. (2016). High-throughput discovery of novel developmental phenotypes.
293 *Nature*, 537(7621):508–514.
- 294 Doran, A. G., Wong, K., Flint, J., Adams, D. J., Hunter, K. W., and Keane, T. M. (2016). Deep genome
295 sequencing and variation analysis of 13 inbred mouse strains defines candidate phenotypic alleles,
296 private variation and homozygous truncating mutations. *Genome Biology*, 17(1):167.
- 297 Eilbeck, K., Lewis, S. E., Mungall, C. J., Yandell, M., Stein, L., Durbin, R., and Ashburner, M. (2005).
298 The Sequence Ontology: a tool for the unification of genome annotations. *Genome Biology*, 6(5):R44.
- 299 Grupe, A., Germer, S., Usuka, J., Aud, D., Belknap, J. K., Klein, R. F., Ahluwalia, M. K., Higuchi, R.,
300 and Peltz, G. (2001). In silico mapping of complex disease-related traits in mice. *Science (New York,
301 N.Y.)*, 292(5523):1915–1918.
- 302 Hunt, S. E., McLaren, W., Gil, L., Thormann, A., Schuilenburg, H., Sheppard, D., Parton, A., Armean,
303 I. M., Trevanion, S. J., Flicek, P., and Cunningham, F. (2018). Ensembl variation resources. *Database*,
304 2018. bay119.
- 305 Ivandic, B. T., Qiao, J. H., Machleder, D., Liao, F., Drake, T. A., and Lusic, A. J. (1996). A locus on
306 chromosome 7 determines myocardial cell necrosis and calcification (dystrophic cardiac calcinosis) in
307 mice. *Proceedings of the National Academy of Sciences of the United States of America*, 93(11):5483–
308 5488.
- 309 Ivandic, B. T., Utz, H. F., Kaczmarek, P. M., Aherrahrou, Z., Axtner, S. B., Klepsch, C., Lusic, A. J.,
310 and Katus, H. A. (2001). New Dyscalc loci for myocardial cell necrosis and calcification (dystrophic
311 cardiac calcinosis) in mice. *Physiological Genomics*, 6(3):137–144.
- 312 Jeong, E., Choi, H. K., Park, J. H., and Lee, S. Y. (2018). STAC2 negatively regulates osteoclast formation
313 by targeting the RANK signaling complex. *Cell Death and Differentiation*, 25(8):1364–1374.
- 314 Keane, T. M., Goodstadt, L., Danecek, P., White, M. A., Wong, K., Yalcin, B., Heger, A., Agam, A.,
315 Slater, G., Goodson, M., Furlotte, N. A., Eskin, E., Nellåker, C., Whitley, H., Cleak, J., Janowitz, D.,
316 Hernandez-Pliego, P., Edwards, A., Belgard, T. G., Oliver, P. L., McIntyre, R. E., Bhomra, A., Nicod,
317 J., Gan, X., Yuan, W., van der Weyden, L., Steward, C. A., Bala, S., Stalker, J., Mott, R., Durbin, R.,
318 Jackson, I. J., Czechanski, A., Guerra-Assunção, J. A., Donahue, L. R., Reinholdt, L. G., Payseur,
319 B. A., Ponting, C. P., Birney, E., Flint, J., and Adams, D. J. (2011). Mouse genomic variation and its
320 effect on phenotypes and gene regulation. *Nature*, 477(7364):289–294.
- 321 Kim, H.-G., Kim, H.-T., Leach, N. T., Lan, F., Ullmann, R., Silahatoglu, A., Kurth, I., Nowka, A.,
322 Seong, I. S., Shen, Y., Talkowski, M. E., Ruderfer, D., Lee, J.-H., Glotzbach, C., Ha, K., Kjaergaard, S.,
323 Levin, A. V., Romeike, B. F., Kleefstra, T., Bartsch, O., Elsea, S. H., Jabs, E. W., MacDonald, M. E.,
324 Harris, D. J., Quade, B. J., Ropers, H.-H., Shaffer, L. G., Kutsche, K., Layman, L. C., Tommerup,
325 N., Kalscheuer, V. M., Shi, Y., Morton, C. C., Kim, C.-H., and Gusella, J. F. (2012). Translocations
326 disrupting PHF21A in the Potocki-Shaffer-syndrome region are associated with intellectual disability
327 and craniofacial anomalies. *American Journal of Human Genetics*, 91(1):56–72.
- 328 McLaren, W., Gil, L., Hunt, S. E., Riat, H. S., Ritchie, G. R. S., Thormann, A., Flicek, P., and Cunningham,
329 F. (2016). The Ensembl Variant Effect Predictor. *Genome Biology*, 17(1):122.
- 330 Meehan, T. F., Conte, N., West, D. B., Jacobsen, J. O., Mason, J., Warren, J., Chen, C.-K., Tudose,
331 I., Relac, M., Matthews, P., Karp, N., Santos, L., Fiegel, T., Ring, N., Westerberg, H., Greenaway,
332 S., Sneddon, D., Morgan, H., Codner, G. F., Stewart, M. E., Brown, J., Horner, N., International
333 Mouse Phenotyping Consortium, Haendel, M., Washington, N., Mungall, C. J., Reynolds, C. L.,
334 Gallegos, J., Gailus-Durner, V., Sorg, T., Pavlovic, G., Bower, L. R., Moore, M., Morse, I., Gao, X.,
335 Tocchini-Valentini, G. P., Obata, Y., Cho, S. Y., Seong, J. K., Seavitt, J., Beaudet, A. L., Dickinson,
336 M. E., Herault, Y., Wurst, W., de Angelis, M. H., Lloyd, K. C. K., Flenniken, A. M., Nutter, L. M. J.,
337 Newbigging, S., McKerlie, C., Justice, M. J., Murray, S. A., Svenson, K. L., Braun, R. E., White,
338 J. K., Bradley, A., Flicek, P., Wells, S., Skarnes, W. C., Adams, D. J., Parkinson, H., Mallon, A.-M.,
339 Brown, S. D. M., and Smedley, D. (2017). Disease model discovery from 3,328 gene knockouts by
340 The International Mouse Phenotyping Consortium. *Nature Genetics*, 49(8):1231–1238.
- 341 Meng, H., Vera, I., Che, N., Wang, X., Wang, S. S., Ingram-Drake, L., Schadt, E. E., Drake, T. A., and
342 Lusic, A. J. (2007). Identification of Abcc6 as the major causal gene for dystrophic cardiac calcification
343 in mice through integrative genomics. *Proceedings of the National Academy of Sciences of the United
344 States of America*, 104(11):4530–4535.
- 345 Mulligan, M. K., Mozhui, K., Prins, P., and Williams, R. W. (2017). GeneNetwork: A Toolbox for
346 Systems Genetics. *Methods in Molecular Biology (Clifton, N.J.)*, 1488:75–120.

- 347 Uhl, E. W. and Warner, N. J. (2015). Mouse Models as Predictors of Human Responses: Evolutionary
348 Medicine. *Current Pathobiology Reports*, 3(3):219–223.
- 349 Wade, C. M., Kulbokas, E. J., Kirby, A. W., Zody, M. C., Mullikin, J. C., Lander, E. S., Lindblad-Toh, K.,
350 and Daly, M. J. (2002). The mosaic structure of variation in the laboratory mouse genome. *Nature*,
351 420(6915):574–578.
- 352 Yates, A., Beal, K., Keenan, S., McLaren, W., Pignatelli, M., Ritchie, G. R. S., Ruffier, M., Taylor,
353 K., Vullo, A., and Flicek, P. (2014). The Ensembl REST API: Ensembl Data for Any Language.
354 *Bioinformatics*, 31(1):143–145.
- 355 Zimmerman, H., Yin, Z., Zou, F., and Everett, E. T. (2019). Interfrontal Bone Among Inbred Strains of
356 Mice and QTL Mapping. *Frontiers in Genetics*, 10:291.